Journal of Power Sources 396 (2018) 491–497

Contents lists available at ScienceDirect

Journal of Power Sources

journal homepage: www.elsevier.com/locate/jpowsour

Electrochemical and structural investigation of Mg-doped $Li_3V_{(2-2x/3)}Mg_x(PO_4)_3$

Soojeong Kim[a], Zhengxi Zhang[b], Senlin Wang[b], Li Yang[b], James E. Penner-Hahn[a,c,*], Aniruddha Deb[a,**]

[a] Department of Chemistry, University of Michigan, Ann Arbor, MI 48109, United States
[b] School of Chemistry and Chemical Technology, Shanghai Jiao Tong University, Shanghai 200240, PR China
[c] Program in Biophysics, University of Michigan, Ann Arbor, MI 48109, United States

HIGHLIGHTS

- Mg doped LVP with sequential two-phase electrochemical transformation.
- Two phase electrochemical behavior is not representative of the bulk material.
- Shows a significant kinetic lag between the surface and bulk electrochemistry.
- Mg doping has been shown to improve conductivity.
- Mg doped samples form a tetrahedral-like V^{5+}.

GRAPHICAL ABSTRACT

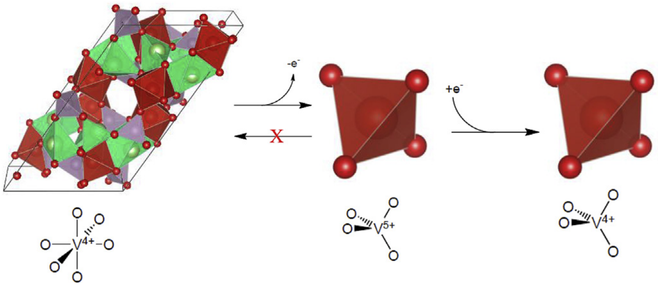

ARTICLE INFO

Keywords:
Mg doped LVP
In-situ x-ray absorption
Li-ion battery
Cathode materials

ABSTRACT

X-ray absorption spectroscopy was used to characterize the local structural environment of the vanadium ions in Mg doped $Li_3V_{(2-2x/3)}Mg_x(PO_4)_3$; x = 0.15, 0.30, 0.45, (LVP) in a functioning battery. For all three compositions the x-ray absorption near-edge structure spectra show evidence for only two spectroscopically distinguishable species when the potential is cycled between 3 and 4.5 V. These are attributed to octahedral V^{3+} and V^{4+} in LVP. If the potential is increased above 4.5 V a third species that is consistent with V^{5+} in a distorted, possibly tetrahedral environment is formed. For x = 0.30 and x = 0.45 this species disappears when the potential is lowered. In contrast, for x = 0.15 a fourth species is formed on reduction. This new species is consistent with V^{4+} in a distorted tetrahedral environment and may explain the loss of capacity in the 15% sample during cycling. Although the potential shows discrete plateaus, consistent with formation of mixed-valence species, these are not seen in the x-ray absorption. Rather, we see apparent deviations from Faraday's law that are consistent with a lag in oxidation of the bulk vanadium.

The rising demands of the electric and hybrid vehicles is pushing the demand for new cathode materials with higher energy storage and power delivery characteristics [1,2]. $Li_3V_2(PO_4)_3$ (LVP) based on phosphate polymerization has recently been extensively studied as one candidate for new cathode materials due to its high redox potential and large lithium ion diffusion channels. All three lithium ions can be readily deintercalated giving a high theoretical capacity of 197 mAh g^{-1} [3], and LVP has both good thermal stability and relatively low environmental impact [4–7]. The charge-discharge profile for LVP shows four well-defined redox plateaus at around 3.62, 3.68, 4.08, and

---

[*] Corresponding author. Program in Biophysics, University of Michigan, Ann Arbor, MI 48109, United States.
[**] Corresponding author.
E-mail address: debani@umich.edu (A. Deb).

https://doi.org/10.1016/j.jpowsour.2018.06.032
Received 12 March 2018; Received in revised form 6 June 2018; Accepted 7 June 2018
0378-7753/ © 2018 Elsevier B.V. All rights reserved.

4.55 V. These first three have been attributed [8,9] to $Li_3V_2(PO_4)_3 \rightarrow Li_{2.5}V_2(PO_4)_3$; $Li_{2.5}V_2(PO_4)_3 \rightarrow Li_2V_2(PO_4)_3$; and $Li_2V_2(PO_4)_3 \rightarrow LiV_2(PO_4)_3$; respectively, based both on charge quantitation (the plateaus have capacities in a ratio of ~1:1:2, corresponding to formal oxidation state transitions of $V^{+3} \rightarrow V^{+3.25}$; $V^{+3.25} \rightarrow V^{+3.5}$; and $V^{+3.5} \rightarrow V^{+4}$) and on neutron diffraction and ^{7}Li NMR characterization of chemically-prepared mixed valence species [8]. The fourth plateau presumably represents $LiV_2(PO_4)_3 \rightarrow V_2(PO_4)_3$ with a formal oxidation state change of $V^{+4} \rightarrow V^{+4.5}$ and, as expected, a capacity that approximately matches the third plateau. LVP has gained a great deal of attention due to its high extraction and insertion voltage, a high theoretical capacity of 197 mAh g^{-1} for the complete removal of the three Li^+ ions, a high diffusion coefficient of 10^{-9} to 10^{-10} cm^2s^{-1} [10–12]. The main disadvantages of LVP, which have been the attention for numerous studies, are its low intrinsic electronic conductivity (~2.4×10^{-7} s cm^{-1}), its low ionic conductivity and capacity fading for voltages greater than 4.6 V, which has been the main hindrance for its practical application [13–15]. Among the methods that have been explored to improve the conductivity of LVP are: coating the LVP with a thin layer of carbon nano-particles [16,17]; reducing the LVP particle size [18–21]; controlling particle morphology [22–25]; and doping metal ions such as Mg^{2+}, Cr^{3+}, Ti^{4+} or Fe^{3+} into the LVP crystal lattice [26–37]. Recent investigations have shown that doping Al^{3+} at the V site can improve the material utilization and lower the capacity fade [4], while Ti^{4+} doping at the V site improved the conductivity and cycling performance [38], and Mg^{2+} doping at the V site improved the high rate discharge performance of LVP [39,40].

Here we use *in operando* x-ray absorption to investigate the effect of Mg^{2+} doping on the vanadium sites in doped LVP during electrochemical cycling. Previous studies of electrochemical performance [40] showed that 15% and 30% Mg^{2+} doped LVP had similar electrochemical properties, while 45% Mg^{2+} doped LVP had enhanced capacity, but decreased retention as compared to 30% doped. The 30% doped system shows the highest discharge capacity, with 91.4% (1C) capacity retention after 100 cycles [40]. Present results allow us to directly relate the vanadium oxidation state with electrochemical potential and to characterize at the atomic level the mechanism of high-potential inactivation.

1. Experimental

1.1. Synthesis and characterization

Hexanedioic acid ($C_6H_{10}O_4$) was used as the chelating agent for preparing Mg-doped LVP composite electrodes. V_2O_5 and oxalic acid in a stoichiometric ratio of 1:3 were dissolved in deionized water and then stirred at 70 °C until dissolved. A stoichiometric mixture of $NH_4H_2PO_4$, Li_2CO_3, $Mg(CH_3COO)_2$ and $C_6H_{10}O_4$ was then added to the resulting blue solution. A gel was formed after stirring this solution for 4 h in air at a temperature of 100 °C. This gel was then heated to 350 °C in a nitrogen atmosphere for 4 h in order to allow the NH_3 and H_2O to escape. The resultant product was then heated under nitrogen at 750 °C for another 4 h. The phase purity of the product was characterized using X-ray diffraction (XRD) measurements (see Fig. S1) using a Rigaku D/max-2200/PC75 diffractometer. The Mg-doped LVP shows a monoclinic phase with a space group of P21/n (see Fig. S1). The morphology of the sample was analyzed by field emitting scanning electron microscopy (FE-SEM, JEOL JSM-7401F). It can be seen (Fig. S2) that the particles of the sample merge with each other forming a porous network [40]. This microstructure is beneficial, as it allows easy penetration of the electrolyte into the positive material, resulting in good electronic contact among the composite particles. A portion of each sample was used to measure the long-term capacity loss during cycling. These data (Fig. S3) show that all three levels of Mg^{2+} doping give a modest (~20%) improvement in capacity relative to the undoped parent compound, with no significant change in capacity loss over 100 cycles.

1.2. In situ X-ray absorption spectroscopy

The experiments were performed using a complete Li / $Li_3V_{(2-2x/3)}Mg_x(PO_4)_3$ half-cell. A special electrochemical *in situ* XAS cell was used for these experimental investigations; for a complete detailed design and assembly, the reader is referred to Deb et al. [41] The electrodes used in the *in situ* experiments were fabricated from an intimate mixture of $Li_3V_{(2-2x/3)}Mg_x(PO_4)_3$ powder comprised of 80% by weight of the total electrode with 10% polyvinylidene difluoride polymer binder (Kynar), 10% compressed acetylene black in N-methyl-2-pyrrolidinone (NMP). The NMP was then evaporated at 60 °C for 6 h and finally the electrodes were dried at 120 °C for another 6 h. The thickness of the active mass on the electrode was ~100 μm. The electrochemical cell was assembled in an argon filled glove box. The separator was placed on top of the working LVP electrode soaked in 1 M $LiPF_6$ electrolyte, dissolved in 50 wt % ethylene carbonate (EC), and 50 wt % dimethylcarbonate (DMC) obtained as a solution from BASF. A lithium foil counter electrode was punched to give a disk with an outer diameter of 14 mm and an inner diameter of 8 mm and placed on top of the separator which was soaked with electrolyte. Kapton film (25.4 μm thickness) was utilized as the X-ray window for this *in situ* electrochemical reaction cell.

During the XAS measurements (each scan ~ 40 min) the electrochemical cell was cycled continuously using a Princeton Applied Research Versastat potentiostat. Cycling was performed using two different sets of cut-off voltages: first, each electrode was cycled from 3 to 4.5 V and then back to 3 V (Cycle **A**); then, each electrode was cycled from 3 to 4.8 V, but on discharge, the voltage was decrease from 4.8 to 2.0 V (Cycle **B**). In all cases, electrodes were cycled with a rate of 0.1C (1C = 140 mAh g^{-1}). At the end of each charge and discharge half-cycle, additional XAS scans were performed while the electrode was equilibrated, which allowed us to track the changes in the electrode while it was allowed to equilibrate.

The *in-situ* measurements were performed at the bending magnet beamline station D of the DND-CAT (Sector 5), at the Advanced Photon Source, using a water cooled Si(111) double crystal monochromator. The energy resolution of the monochromatic beam was ~1.0 eV [42]. A beam size of 0.3 × 4 mm^2 was used for these transmission mode measurements with an incident photon flux of ~10^{10} photon/s. A third ion chamber was placed after the sample and a reference vanadium foil was placed between the second and third ion chambers to provide an internal reference. The first inflection point of the vanadium foil was defined as 5465 eV. The monochromator was scanned from 200 eV below to 800 eV above the vanadium K-absorption edge. Data was recorded with a step size of 5 eV below 5460 eV, 0.25 eV step size for the pre-edge region (5460–5480 eV), for the near edge region (5480–5560 eV) it was 0.5 eV, and in the EXAFS region (5560–6265 eV) a step size of 0.05 $Å^{-1}$ was used. The data was integrated for 1 s per step in the pre-edge, 1.5 s per step for the near edge region and 1.5–25 s per step (k^3 weighted) for the EXAFS region resulting to around 40 min for each scan. During the cycling of the cell, additional XANES scans were taken while the working electrode was allowed to equilibrate at the cut-off voltages (3.0 V, 4.5 V, 4.8 V and 2.0 V).

1.3. Data analysis

EXAFS data analysis was performed using the EXAFSPAK package [43]. A background for the pre-edge and a cubic spline background for the EXAFS were subtracted, and the EXAFS oscillations were normalized to the appropriate Victoreen function modeling the absorption decrease above the edge [44]. The resulting $\chi(k)$ function was weighted by k^3 to account for the damping of oscillations with increasing k. The radial structure functions were calculated by Fourier transformation of $k^3\chi(k)$ using a k-range of 1.5–11.5 $Å^{-1}$. The EXAFS data was fit in EXAFSPAK using FEFF9 [45] to calculate *ab initio* phase and amplitude parameters based on the crystal structure of LVP.

Download English Version:

https://daneshyari.com/en/article/7724890

Download Persian Version:

https://daneshyari.com/article/7724890

Daneshyari.com